1-D and 2-D Homoleptic Dicyanamide Structures, $[Ph_4P]_2\{Co^{II}[N(CN)_2]_4\}$ and $[Ph_4P]\{M[N(CN)_2]_3\}$ (M = Mn, Co)⊥

James W. Raebiger,† Jamie L. Manson,‡ Roger D. Sommer,§ Urs Geiser,‡ Arnold L. Rheingold,§ and Joel S. Miller*,†

Department of Chemistry, University of Utah, 315 S 1400 E, Salt Lake City, Utah 84112-0850, Materials Science Division, Argonne National Laboratory, 9700 South Cass Avenue, Argonne, Illinois 60439-4831, and Department of Chemistry, University of Delaware, Newark, Delaware 19716

Received December 6, 2000

The homoleptic complexes $[Ph_4P]_2\{Co[N(CN)_2]_4\}$ and $[Ph_4P]\{M[N(CN)_2]_3\}$ [M = Co, Mn] have been structurally as well as magnetically characterized. The complexes containing $\{M[N(CN)_2]_4\}^{2-}$ form 1-D chains, which are bridged via a common dicyanamide ligand in $\{M[N(CN)_2]_3\}^-$ to form a 2-D structure. The five-atom $[NCNCN]^-$ bridging ligands lead to weak magnetic coupling along a chain. The six $[NCNCN]^-$ ligands lead to a $^4T_{1g}$ ground state for Co(II) which has an unquenched spin−orbit coupling that is reflected in the magnetic properties. Long-range magnetic ordering was not observed in any of these materials.

Introduction

The magnetic behavior of homo-[1−6] and heteroleptic[7] complexes with the dicyanamide ligand, $[N(CN)_2]^-$, has received considerable recent attention. Homoleptic complexes with divalent transition metals, $M^{II}[N(CN)_2]_2$ (M = Cr,[1] Mn,[1,2] Fe,[3] Co,[3−5] Ni[3−5]), magnetically order as ferro- or weak antiferromagnets with $T_c \leq 47$ K. In contrast, heteroleptic complexes have yet to be reported to magnetically order. In the homoleptic compounds, $[N(CN)_2]^-$ is tricoordinate, bridging three different metal sites, while in the heteroleptic compounds, dicyanamide bridges two metal sites exclusively via the nitriles. To further establish the magnetic structure−function relationship as well as identify new magnetically ordered materials, we investigated three new homoleptic compounds, $[Ph_4P]_2\{Co[N(CN)_2]_4\}$ (**1**) and $[Ph_4P]\{M[N(CN)_2]_3\}$ [M = Co (**2**), Mn (**3**)].

The chemistry of dicyanamide as a ligand has been explored for many years. Köhler and co-workers published a series of papers in the 1960s and 1970s describing transition metal dicyanamide complexes. They reported the preparation of several cobalt dicyanamde complexes including $(Ph_3MeAs)\{Co[N(CN)_2]_3\}$.[8] We have utilized the tetraphenylphosphonium salt of dicyanamide as a starting material to prepare **1**−**3**.

Experimental Section

$Co(NO_3)_2 \cdot 6H_2O$ and $MnCl_2 \cdot 4H_2O$ (Baker) were used as purchased. $[Ph_4P][N(CN)_2]$ and $K[N(CN)_2]$ were synthesized by metathesis from $Ag[N(CN)_2]$. Infrared spectra were recorded on a Bio-Rad FTS-40 FT-IR spectrometer with samples prepared as Nujol mulls. Absorption spectra were recorded on a Hewlett-Packard 8452A diode-array spectrophotometer. Magnetic measurements were taken on a Quantum Design MPMS-5T magnetometer as previously described.[9]

$[Ph_4P]_2\{Co[N(CN)_2]_4\}$ (1). A solution of 0.35 g (1.2 mmol) of $Co(NO_3)_2 \cdot 6H_2O$ dissolved in 30 mL of acetone was added to a stirred solution of 0.25 g (2.4 mmol) of $K[N(CN)_2]$ and 0.97 g (2.4 mmol) of $(Ph_4P)[N(CN)_2]$ in 120 mL of acetone. The resulting dark blue solution was stirred for 5 min and then filtered. The filtrate was reduced to 30 mL, and ether diffusion produced a mixture of white and pink needles. The mixture was washed with 95% ethanol to remove the white crystals and produce 180 mg (15%) of homogeneous pink needles.

$[Ph_4P]\{Co[N(CN)_2]_3\}$ (2). A solution of 0.30 g (1.0 mmol) of $Co(NO_3)_2 \cdot 6H_2O$ dissolved in 30 mL of acetone was added to a stirred solution of 0.22 g (2.0 mmol) of $K[N(CN)_2]$ and 0.42 g (1.0 mmol) of $(Ph_4P)[N(CN)_2]$ in 120 mL of acetone. The resulting dark blue solution was stirred for 1 h and then filtered. The filtrate was reduced to 20 mL, and ether diffusion produced 75 mg (10%) of pink block crystals.

$[Ph_4P]\{Mn[N(CN)_2]_3\}$ (3). A solution of 0.186 g (0.94 mmol) of $MnCl_2 \cdot 4H_2O$ in 10 mL of ethanol was slowly added to a solution of 0.800 g (1.97 mmol) of $[Ph_4P][N(CN)_2]$ in 10 mL of CH_2Cl_2 to give a colorless solution. The reaction mixture was allowed to slowly evaporate

⊥ Dedicated to Alan L. Balch on the occasion of his 60th birthday.
† University of Utah.
‡ Argonne National Laboratory.
§ University of Delaware.

(1) Manson, J. L.; Kmety, C. R.; Epstein, A. J.; Miller, J. S. *Inorg. Chem.* **1999**, *38*, 2552.
(2) Batten, S. R.; Jensen, P.; Kepert, C. J.; Kurmoo, M.; Moubaraki, B.; Murray, K. S.; Price, D. J. *J. Chem. Soc., Dalton Trans.* **1999**, 2987.
(3) Kurmoo, M.; Kepert, C. J. *New J. Chem.* **1998**, 1515.
(4) Batten, S. R.; Jensen, P.; Moubaraki, B.; Murray, K. S.; Robson, R. *Chem. Commun.* **1998**, 439.
(5) Manson, J. L.; Kmety, C. R.; Huang, Q.; Lynn, J. W.; Bendele, G. M.; Pagola, S.; Stephens, P. W.; Liable-Sands, L. M.; Rheingold, A. L.; Epstein, A. J.; Miller, J. S. *Chem. Mater.* **1998**, *10*, 2552.
(6) Köhler, H.; Kolbe, A.; Lux, G. *Z. Anorg. Allg. Chem.* **1977**, *428*, 103.
(7) E.g.: Manson, J. L.; Arif, A. M.; Incarvito, C. D.; Liable-Sands, L. M.; Rheingold, A. L.; Miller, J. S. *J. Solid State Chem.* **1999**, *145*, 369. Manson, J. L.; Incarvito, C. D.; Rheingold, A. L.; Miller, J. S. *J. Chem. Soc., Dalton Trans.* **1998**, 3705. Manson, J. L.; Arif, A. M.; Miller, J. S. *Mol. Cryst. Liq. Cryst. Sci. Technol., Sect. A* **1999**, *334*, 605. Manson, J. L.; Incarvito, C. D.; Arif, A. M.; Rheingold, A. L.; Miller, J. S. *J. Mater. Chem.* **1999**, *9*, 979. Marshall, S. M.; Incarvito, C. D.; Rheingold A. L.; Manson, J. L.; Miller, J. S. *Inorg. Chem.* **2000**, *39*, 1969. Claramunt, A.; Escuer, A.; Mautner, F. A.; Sanz, N.; Vicente, R. *J. Chem. Soc., Dalton Trans.* **2000**, 2627. Batten, S. R.; Harris, A. R.; Jensen, P.; Murray, K. S.; Ziebell, A. *J. Chem. Soc., Dalton Trans.* **2000**, 3829. Jensen, P.; Batten, S. R.; Moubaraki, B.; Murray, K. S. *Chem. Commun.* **2000**, 793. van Albada, G. A.; Quiroz-Castro, M. E.; Mutikainen, I.; Turpeinen, U.; Reedijk, J. *Inorg. Chim. Acta* **2000**, *298*, 221.
(8) Köhler, H.; Seifert, B. *Z. Anorg. Allg. Chem.* **1966**, *344*, 63.
(9) Brandon, E. J.; Rittenberg, D. K.; Arif, A. M.; Miller, J. S. *Inorg. Chem.* **1998**, *37*, 3376.

10.1021/ic001379t CCC: $20.00 © 2001 American Chemical Society
Published on Web 04/07/2001

Table 1. Crystallographic Data for $[Ph_4P]_2\{Co[N(CN)_2]_4\}$, **1**, and $[Ph_4P]\{M[N(CN)_2]_3\}$, M = Co, **2**, Mn, **3**

	1	**2**	**3**
chem formula	$C_{56}H_{40}CoN_{12}P_2$	$C_{30}H_{20}CoN_9P$	$C_{30}H_{20}MnN_9P$
fw (g mol^{-1})	1001.87	596.45	592.46
space group	*C*2/*c*	*P*2/*n*	*P*2/*n*
a (Å)	23.3789(10)	13.4354(10)	13.3903(6)
b (Å)	7.5684(3)	7.4426(5)	7.5745(3)
c (Å)	28.3778(12)	14.1556(10)	14.3935(6)
β (deg)	105.6210(10)	101.0870(10)	99.663(2)
V (Å^3)	4835.7(3)	1389.06(17)	1439.15(10)
Z	4	2	2
T (K)	173(2)	173(2)	295(2)
λ (Å)	0.71073	0.71073	0.71073
D_{calc} (g cm^{-3})	1.376	1.426	1.367
μ (cm^{-1})	47.4	71.3	55.1
R^a	0.0323	0.0533	0.0344
R_w [b]	0.0817	0.0986	0.0894

[a] $R = \sum[|F_o| - |F_c|]/\sum|F_o|$. [b] $R_w = [\sum w[|F_o| - |F_c|]^2/\sum w|F_o|^2]^{1/2}$.

at room temperature for 3 days, at which time large colorless blocks of $[Ph_4P]\{Mn[N(CN)_2]_3\}$ had grown. The crystals were collected via vacuum filtration and air-dried to give 0.249 g (45%) of colorless block crystals.

Results and Discussion

The known homoleptic compounds, $M^{II}[N(CN)_2]_2$, are prepared from aqueous solution.[1−6] In order to achieve different products, $[Ph_4P][N(CN)_2]$ was used as a source of dicyanamide in the acetone (Co^{II}) and CH_2Cl_2/ethanol (Mn^{II}). The products $[Ph_4P]_2\{Co[N(CN)_2]_4\}$ (**1**) and $[Ph_4P]\{Co[N(CN)_2]_3\}$ (**2**) were produced as large pink crystals by ether diffusion, and $[Ph_4P]\{Mn[N(CN)_2]_3\}$ (**3**) was produced by solvent evaporation as large, colorless crystals. Related compounds have been prepared by Köhler and co-workers in their investigations of dicyanamide complexes. They reported a number of homoleptic complexes including $\{M[N(CN)_2]_4\}^{2-}$ (M = Pd, Pt)[10] and $\{Ni[N(CN)_2]_3\}^-$,[11] as monomeric species with terminal dicyanamide ligands. They also reported several cobalt compounds including $[Ph_3MeAs]\{Co[N(CN)_2]_3\}$ (**4**) and $[Ph_3MeAs]_2\{Co[N(CN)_2]_4\}$[8] (**5**) as octahedral compounds in the solid state and tetrahedral in solution; however, neither their structure nor their temperature-dependent magnetic properties were reported, and data supporting these formulations were limited. Compounds **1** and **2** have properties similar, but not identical, to those of **4** and **5**.

The structures of **1**−**3** have been determined from single-crystal X-ray analyses; crystallographic data are summarized in Table 1. In each case the M^{II} (M = Mn, Co) is hexacoordinate and surrounded by six dicyanamide ligands nitrile-bound to M, with two pair of dicyanamides bridging adjacent M's, i.e., **6*a***. These **6*a*** M−N distances average 2.163 and 2.116 Å for **1** and **2**, respectively, and average 2.113 Å for **3**. Each M is also coordinated to two additional dicyanamides, **6*b***, with **6*b*** M−N distances of 2.083, 2.157, 2.277 Å for **1**, **2**, and **3**, respectively. These values are consistent with previously reported M−N distances, e.g., 2.101 and 2.161 Å for $Co[N(CN)_2]_2$.[5]

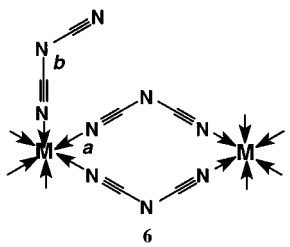

6

Compound **1** forms a 1-D chain with the two terminal dicyanamide ligands per Co, **6*b***, Figure 1. The terminal $[N(CN)_2]^-$ ligands of each chain interdigitate with those from adjacent chains. In contrast, **2** and **3** are isostructural and have a 2-D network, as typified by **2**, Figure 2. For **2** and **3** the terminal $[N(CN)_2]^-$ ligands on one chain bridge to an adjacent chain, hence the stoichiometry for **1** is $\{Co^{II}[N(CN)_2]_4\}^{2-}$, while it is $\{M^{II}[N(CN)_2]_3\}^-$ for **2** and **3**. In each case the $[Ph_4P]^+$ cations lie between the chains or sheets.

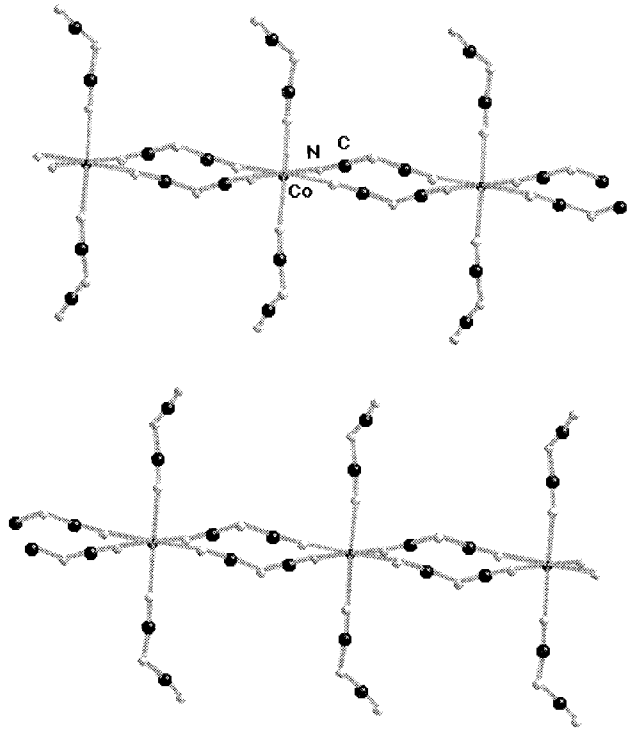

Figure 1. Chain (1-D) network structure of $[Ph_4P]_2\{Co[N(CN)_2]_4\}$, **1**. The cations have been omitted for clarity.

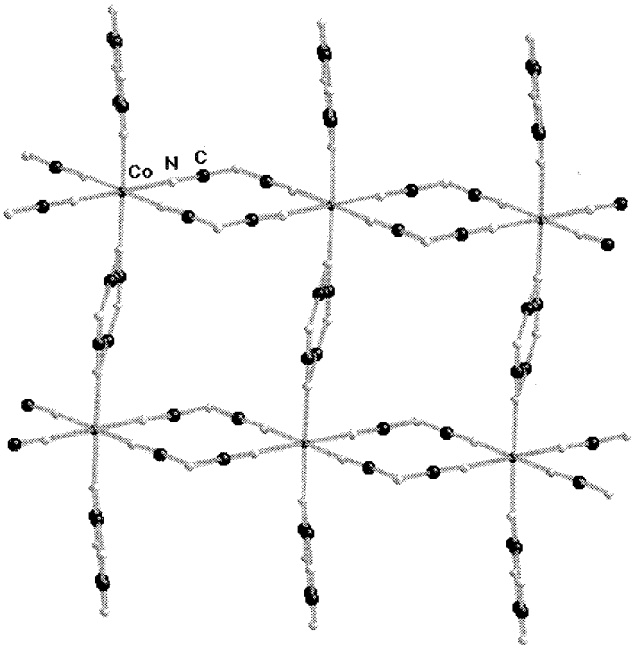

Figure 2. Layered (2-D) network structure of $[Ph_4P]\{Co[N(CN)_2]_3\}$, **2** (**3** is isomorphous). The cations have been omitted for clarity.

Compound **1** appears to be a precursor for the formation of the sheets in compound **2**. The loss of $[Ph_4P][N(CN)_2]$ per Co would result in the bridging of the chains in **1** to form the sheets of **2**. This is observed as recrystallization of **1** from acetone/

ether produces the pink block crystals of **2** as confirmed by unit cell analysis and infrared spectroscopy.

Linear chain structured **1** has IR ν_{CN} stretching absorptions at 2277 (s), 2229 (w), 2222 (m), and 2162 (vs) cm^{-1}. In contrast, **2** has ν_{CN} absorptions at 2291 (s), 2246 (m), 2232 (w), and 2175 (vs) cm^{-1}, and **3** has similar absorptions at 2292 (s), 2240 (m), 2224 (w), 2177 (vs) and 2165 (vs) cm^{-1}. Unfortunately, there are no assignments for these absorptions, and absorptions of **2** do not correspond to 2259, 2246, 2200, and 2170 cm^{-1} reported for $[Ph_3MeAs]\{Co[N(CN)_2]_3\}$ (**4**),[8] suggesting that it may be of different stoichiometry.

The pink crystals of **2** are partially soluble in both dichloromethane and acetone. Addition of 5 equiv of $[Ph_4P][N(CN)_2]$ to the crystals in acetone leads to complete dissolution of **2**, forming a dark blue solution. The UV−visible absorption spectrum of the resultant solution has two absorptions at 16 400 cm^{-1} ($\epsilon = 1000\ cm^{-1}\ M^{-1}$) and 16 700 cm^{-1} (1020 $cm^{-1}\ M^{-1}$) and a shoulder at 17 500 cm^{-1} ($\epsilon = 700\ cm^{-1}\ M^{-1}$). The peak positions are the same in neat acetone and dichloromethane (when some solid remains undissolved), indicating that the soluble species is the same in either solvent. The peaks correspond to the absorptions for tetrahedral Co^{II}, which has features between 14 000 and 17 000 cm^{-1} assigned to the $^4A_2(F) \rightarrow {}^4T_1(F)$ transition (octahedral Co^{II} has peaks at 19 600 and 21 600 cm^{-1} assigned to the $^4T_{1g}(F) \rightarrow {}^4A_{2g}(F)$ and $^4T_{1g}(F) \rightarrow {}^4T_{1g}(P)$ transitions, respectively).[12] This also corresponds to the reflectance spectrum obtained for β-$Co[N(CN)_2]_2$, a network structure proposed to have tetrahedral symmetry.[12] Therefore, it seems likely that in solution, and only in solution, tetrahedral $\{Co[N(CN)_2]_4\}^{2-}$ forms. It is proposed to form via the equilibrium in eq 1 in an excess of dicyanamide.

$$\{Co^{II}[N(CN)_2]_3\}^- + [N(CN)_2]^- \leftrightarrows \{Co[N(CN)_2]_4\}^{2-} \quad (1)$$

The temperature dependence of the magnetic susceptibilities of **1**−**3** was measured between 2 and 300 K. **1**−**3** have room temperature moments of 5.14, 5.14, and 5.85 μ_B, respectively. The value for **3** is as expected for uncoupled spin-only $S = {}^5/_2$ Mn^{II}. In contrast, the moments for **1** and **2** substantially exceed the spin-only value of 3.84 μ_B expected for high-spin Co^{II}.

The temperature dependence of the magnetic susceptibility, χ, of $[Ph_4P]_2\{Co[N(CN)_2]_4\}$, **1**, and $[Ph_4P]\{Co[N(CN)_2]_3\}$, **2**, cannot be fit to the Curie−Weiss expression, $\chi \propto [T - \theta]^{-1}$, due to the curvature of $\mu(T)$, Figure 3. High-spin octahedral Co^{II} has a $^4T_{1g}$ ground state and, as a consequence, exhibits unquenched spin−orbit coupling in addition to zero-field splitting, which dominates at low temperature.[13] Unfortunately, no expression accounts for both factors simultaneously. Therefore, the data for **2** were fit with eq 2 (with $x = \lambda/k_BT$) for spin−orbit coupling, λ, of Co^{II}, which dominates above 50 K (Figure 3). The best fit is obtained with values of $A = 1.5$, $k = 1.0$, $\lambda = -170\ cm^{-1}$, and $\nu = 3$, where A is a crystal field parameter ($A = 1.5$ is weak-field limit), k represents electron delocalization ($k = 1.0$ is minimal), λ is the spin−orbit coupling constant ($\lambda = -176\ cm^{-1}$ is the free-ion value), and ν describes the distorted geometrical configurations (ν is proportional to $1/\lambda$). Thus, the fit suggests cobalt ions with slightly distorted octahedral geometry, which is consistent with the crystal structure. The room temperature moment of 5.14 μ_B is close to that expected for the weak-field ion with spin−orbit coupling (5.20 μ_B), with the slightly lower value indicative of the small perturbation from ideal octahedral geometry as is structurally observed.

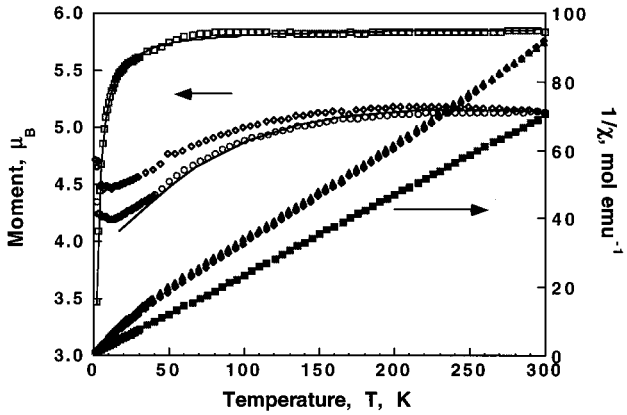

Figure 3. Temperature dependence of the effective moment, $\mu_{eff}(T)$, and reciprocal susceptibility, $1/\chi(T)$, for **1** (◇), **2** (○), and **3** (□), and fit to eq 2 for **2**, and Curie−Weiss equation and eq 3 for **3**.

$$\mu^2 = \frac{\left[\frac{7(3-A)^2x}{5} + \frac{12(A+2)^2}{25A} + \left\{\frac{2(11-2A)^2x}{45} + \frac{176(A+2)^2}{675A}\right\}\exp\left(-\frac{5Ax}{2}\right) + \left\{\frac{(A+5)^2x}{9} - \frac{20(A+2)^2}{27A}\right\}\exp(-4Ax)\right]}{\frac{x}{3}\left[3 + 2\exp\left(-\frac{5Ax}{2}\right) + \exp(-4Ax)\right]} \quad (2)$$

Similar behavior was observed for 1-D compound **1**. However, the susceptibility is higher at low temperature than that of **2**, and the data could not be fit to eq 2. The enhanced susceptibility of **1** with respect to **2** is attributed to a contribution from the interlayer coupling via the five-atom μ-$[NCNCN]^-$ linkages present in **1**, but not **2**. Since models presently cannot account for this coupling in addition to the effect arising from spin−orbit coupling, the data cannot be modeled. Because the octahedral geometry of the Co^{II} ion is similar for both **1** and **2**, their magnetic behavior should be similar. Hence, the less decreasing moment with decreasing temperature of **1** with respect to **2** suggests that their differences must be attributed to their 1- and 2-D structural motifs, **1** consisting of weakly interacting linear chains. The more rapidly decreasing moment of **2** at lower temperatures is in agreement with this hypothesis. At ∼13 K there is an upturn in the susceptibility for both **1** and **2**. The origin of this is unknown; however, AC susceptibility measurements did not reveal a peak; hence, the increase is not due to magnetic ordering. Similar behavior was observed in the compound $Co[C(CN)_3]_2$.[14]

The $\chi(T)$ of **3** can be fit to the Curie−Weiss equation with $g = 1.99(1)$ and $\theta = -3.04(4)$ K, Figure 3. The g value is within experimental error of the expected value of 2.00 for the isotropic Mn^{II} ion. The small θ value reflects a weak antiferromagnetic coupling between the Mn^{II} ions within the 2-D layers. At room temperature, the effective moment, μ_{eff}, has a value of 5.85 μ_B, which is slightly less than the expected spin-only value of 5.92 μ_B for paramagnetic $S = {}^5/_2$ spins. Upon cooling, $\mu_{eff}(T)$ remains invariant until ∼50 K, where it then begins to decrease more rapidly owing to increasing antiferromagnetic correlations. A

(10) Köhler, H.; Jeschke, M.; Wusterhausen, H. *Z. Anorg. Allg. Chem.* **1987**, *549*, 199.
(11) Köhler, H.; Hartung, H.; Golub, A. M. *Z. Anorg. Allg. Chem.* **1974**, *403*, 41.
(12) Figgis, B. N. *Introduction to Ligand Fields*; Wiley Interscience: New York, 1966; Chapter 9.
(13) Mabbs, F. E.; Machin, D. J. *Magnetism and Transition Metal Complexes*; Chapman and Hall: London, 1973; pp 99−100.
(14) Batten, S. R.; Hoskins, B. F.; Moubaraki, B.; Murray, K. S.; Robson, R. *J. Chem. Soc., Dalton Trans.* **1998**, 3705.

value of 3.47 μ_B is obtained at 2 K. At these low temperatures, a small zero-field splitting may also contribute, but it is often too small to be of any significance.

$$\chi_{2D} = 2.91\frac{Ng^2{\mu_B}^2}{k_B T}[1 + C_1x + C_2x^2 + C_3x^3 + C_4x^4 + C_5x^5 + C_6x^6]^{-1} \quad (3)$$

The $\mu_{eff}(T)$ data for **3** were also fit to the 2-D Rushbrooke−Wood model[15] (eq 3) in an effort to ascertain the magnitude of the exchange interaction, giving $g = 1.99(1)$ and $J/k_B = -0.11(1)$ K, Figure 3. This small J value is comparable to that observed for the heteroleptic linear chain compounds $Mn[N(CN)_2]_2(L)_2$ (L = methanol, *N*,*N*-dimethylformamide, pyridine) with $J/k_B = -0.12$ K.[2] Moreover, the expected maximum, as is typical of a 2-D-layered system, was not observed and likely occurs at a lower temperature than could be measured. Similarly, long-range magnetic ordering was not observed above 2 K. The coupling is characteristic of weak antiferromagnetic interactions across the five-atom dicyanamide bridge.

In summary, three homoleptic dicyanamide compounds, namely, 1-D $[Ph_4P]_2\{Co[N(CN)_2]_4\}$ and the 2-D $[Ph_4P]\{M[N(CN)_2]_3\}$ (M = Co, Mn), have been prepared. The structures contain only dicyanamide ligands that bridge through the nitrile nitrogen atoms. Stronger magnetic coupling that leads to magnetic ordering requires bonding via the central amide nitrogen, a motif absent in these compounds. Therefore the lack of low-temperature magnetic ordering is expected. We are currently investigating the solution properties of **2** to determine the stability and utility of the proposed soluble tetrahedral monomer.

Acknowledgment. We acknowledge the support from the U.S. Department of Energy (Grant No. DE FG 03-93ER45504) and U.S. National Science Foundation (Grant No. CHE-9320478). Work performed at Argonne National Laboratory is supported by the Office of Basic Energy Sciences, Division of Materials Science, U.S. Department of Energy under Grant W-31-109-ENG-38.

Supporting Information Available: Crystallographic data in CIF format. This material is available free of charge via the Internet at http://pubs.acs.org.

IC001379T

(15) (a) Rushbrooke, G. S.; Wood, P. J. *J. Mol. Phys.* **1963**, *6*, 409. (b) $x = J/(k_BT)$, N = Avogadro's number, μ_B = Bohr magneton, g = Lande g value, $C_1 = 23.33$, $C_2 = 147.78$, $C_3 = 405.45$, $C_4 = 8171.3$, $C_5 = 64968$, and $C_6 = 15811$.